

Membrane-Derived Fluorinated Radicals Detected by Electron Spin Resonance in UV-Irradiated Nafion and Dow Ionomers: Effect of Counterions and H₂O₂

Marsil K. Kadirov,[†] Admir Bosnjakovic, and Shulamith Schlick*

Department of Chemistry and Biochemistry, University of Detroit Mercy, 4001 West McNichols, Detroit, Michigan 48221

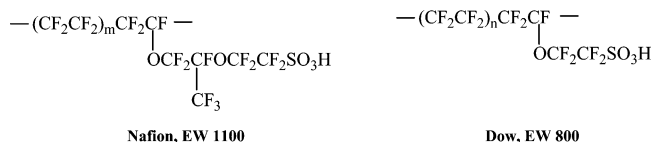
Received: November 2, 2004; In Final Form: February 11, 2005

Electron spin resonance (ESR) spectroscopy was used to detect and identify radicals formed by UV irradiation of Nafion and Dow perfluorinated membranes partially or fully neutralized by Cu(II), Fe(II), and Fe(III). This method allowed the monitoring of ESR signals from the paramagnetic counterions together with the appearance of membrane-derived radical species. The most surprising aspect of this study was the formation of membrane-derived radical species only in the neutralized membranes, and even in the absence of H₂O₂ in the case of Nafion/Cu(II) and Nafion/Fe(III). In Nafion/Cu(II), ESR spectra from radicals exhibiting hyperfine interactions with three equivalent ¹⁹F nuclei (the “quartet”) and with four equivalent ¹⁹F nuclei (the “quintet”) were detected. In Nafion/Fe(II) exposed to H₂O₂ solutions, the formation of Fe(III) was detected. Upon UV irradiation, strong signals from the chain-end radical ROCF₂CF₂• were detected first, followed by the appearance, upon annealing above 200 K, of the quartet signal observed in Nafion/Cu(II). In subsequent experiments with Nafion and Dow membranes neutralized by Fe(III), the ROCF₂CF₂• radicals were formed even in the absence of H₂O₂, indicating that the role of H₂O₂ is oxidation of Fe(II) to Fe(III); moreover, in these systems small amounts of the chain-end radicals were detected even without UV irradiation. This result validates the method used to form the radicals: the role of UV irradiation is to accelerate the formation of a signal that is produced, albeit slowly, even in the dark, and possibly during fuel cell operation. The major conclusion is that cations are involved in degradation processes; the point of attack appears to be at or near the pendant chain of the ionomer. Therefore when studying membrane stability, it is important to consider not only the formation of oxygen radicals, such as HO•, HOO•, and O₂•⁻, that can attack the membrane but also the specific reactivity of counterions.

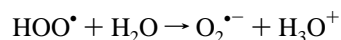
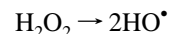
Introduction

The proton exchange membranes (PEMs) used in fuel cells (FCs) are *ionomers*: polymers that were modified to include ions, typically sulfonic groups, -SO₃⁻. In a FC environment, these polymers self-assemble into hydrophobic and hydrophilic domains and allow the transport of H⁺ in one direction only, from the anode to the cathode.¹ The traffic-light role fulfilled by the membrane was first demonstrated by Nafion, the ionomer made by DuPont and shown in Chart 1, which consists of a perfluorinated backbone and pendant chains terminated by sulfonic groups. FCs normally operate at ≈80 °C; important advantages in terms of water management and CO tolerance can be gained by operating at higher temperatures, typically ≈120 °C.² High operating temperatures impose additional requirements in terms of membrane stability in a highly oxidative environment. Even at an operating temperature of 50 °C, evidence for the deterioration of Nafion membranes has been detected by X-ray powder diffraction (XRD) and X-ray photoelectron spectroscopy (XPS); moreover, it was reported that the type of structural damage is different at the anode and at the cathode sides.³ Membrane durability has recently emerged as a major topic of study and a problem that needs to be solved before implementation of FCs as a source of clean energy.

CHART 1: Perfluorinated Membranes, in Acid Form



Reactive oxygen species such as H₂O₂ and HO• are formed during FC operation,^{4,5} and their presence can lead to membrane deterioration. In the laboratory, oxygen radicals can be produced by the Fenton reaction, where the major step is H₂O₂ + Fe(II) → Fe(III) + HO• + HO⁻.⁶ The formation of radical species from the attacked substrate, for instance RH, can occur by H-abstraction, HO• + RH → H₂O + R•; polymer-derived R• radicals can initiate a degradation cascade. Fenton reagents based on Ti(III) instead of Fe(II) have also been used.⁶ An additional method for producing oxygen radicals in the laboratory is photolysis of aqueous solutions of H₂O₂, and the main expected reactions are



DOO• and DO• are expected in UV-irradiated H₂O₂/D₂O solutions. The presence of the radicals was confirmed in our

* Corresponding author: e-mail schlicks@udmercy.edu.

[†] Present address: Institute of Organic and Physical Chemistry, Kazan, Russia.

laboratory by ESR, using a combination of UV irradiation and ESR measurements at low temperature, typically 77 K, followed by gradual annealing of irradiated samples for short intervals (≈ 3 min) above 77 K; in this way ESR signals from radicals HO^\bullet , DO^\bullet , HOO^\bullet , DOO^\bullet , and $\text{O}_2^{\bullet-}$ have been detected.⁷

Currently the stability of FC membranes to oxidation is based on the Fenton test: the polymer is soaked in an aqueous solution of H_2O_2 (3–30%) and FeSO_4 (molar ratio $[\text{Fe(II)}]/[\text{H}_2\text{O}_2] \approx 1/500$); membrane stability is measured in terms of weight loss at a given treatment temperature (ambient to $\approx 80^\circ\text{C}$) as a function of immersion time or in terms of the time required for the membrane to break or to begin dissolving.^{8,9} This test provides no details on reactive intermediates, degradation mechanism, or factors that may affect the extent of structural damage.

The effect of HO^\bullet radicals formed by UV irradiation of H_2O_2 on low molecular weight model sulfonated compounds such as *p*-toluenesulfonic acid has been investigated at ambient temperature as a function of pH in a flow system.¹⁰ It is interesting to note that the radical $-\text{SO}_3^\bullet$ was one of the species formed from the substrate by this method. Recently the presence of radicals formed in situ in a fuel cell (inside the resonator of the X-band ESR spectrometer) was demonstrated by spin trapping.¹¹

The objectives of our recent studies on membrane stability are to achieve a better understanding of the degradation mechanism in PEMs by developing specific treatment protocols in the laboratory. ESR spectroscopy is the major method of study, because of its sensitivity and specificity for the detection of radical species. The major difficulties in this approach are the short lifetimes of the radicals; low temperatures and/or spin trapping techniques can be used to improve the Boltzmann factor, increase the lifetimes, and capture radicals as they form.¹² Recently ESR spectroscopy has been used to detect and identify radicals in Nafion membranes exposed to the Fenton reagent based on Ti(III) ($\text{TiCl}_3 + \text{H}_2\text{O}_2$).¹³ This method has allowed monitoring of the disappearance of the ESR signal from Ti(III) during reaction.¹⁴ The initially detected radical was HOO^\bullet . The disappearance of this radical above 220 K was accompanied by the appearance of a mixture of peroxy radicals TiOO^\bullet and superoxide radicals $\text{O}_2^{\bullet-}$. The $\text{O}_2^{\bullet-}$ radicals were observed only in dry fully neutralized Nafion after treatment, and were stable up to 370 K. A broad signal (line width ≈ 84 G, $g = 2.0023$) appeared in slightly dried samples after ≈ 14 days of exposure to the Fenton reagent and increased in intensity after 92 days; this signal was assigned to fluorinated alkyl radicals, formed by attack of oxygen radicals on the polymer chain.¹³ In this study it was not possible to identify the type of radical formed; the large line width, however, clearly suggested ^{19}F hyperfine splittings, therefore a fluorinated radical fragment.

We present a study of radicals formed in UV-irradiated Nafion neutralized by Cu(II), Fe(II), and Fe(III); some samples were exposed to H_2O_2 solutions prior to UV irradiation. Selected experiments were performed with the Dow perfluorinated membranes, also shown in Chart 1. The major goals were to detect the radicals formed by ESR spectroscopy and to assess the effects of H_2O_2 addition and of specific cations that neutralized the membranes. Cu(II), Fe(II), and Fe(III) are paramagnetic and can be detected by ESR, thus allowing a follow-up of their intensity during the formation of membrane-derived radicals. The above counterions were selected because of their known effect on polymer durability: A dramatic decrease of thermal stability in poly(acrylic acid) containing CuNO_3 was reported;¹⁵ moreover, perfluorinated membranes were less stable when stainless steel end plates were used in

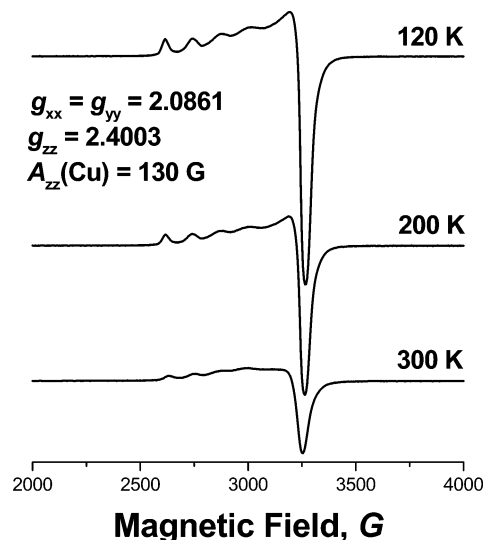


Figure 1. ESR spectra of Cu(II) in Nafion membranes at the indicated temperatures. Degree of membrane neutralization: 2%. The magnetic parameters were read directly from the spectrum measured at 120 K.

FCs, but no deleterious effects were observed with aluminum end plates.¹⁶ To the best of our knowledge the results presented here are the first evidence for the formation of specific membrane-derived radical fragments and suggest that the point of attack is at or near the pendant chain of the ionomer.

Experimental Section

Materials. Nafion membranes with an equivalent weight of 1100 g of polymer/mol of sulfonic groups and a thickness of 0.178 mm were obtained from DuPont. The mean repeat unit of the backbone consisted of 14 CF_2 groups and one CF group; in Chart 1, $m = 6.5$. Aqueous solutions of H_2O_2 (30% and 3% w/v) were from Fisher. The Dow membranes, with an equivalent weight of 800 g of polymer/mol of sulfonic groups ($n = 5.2$) and a thickness of 0.050 mm, were a gift from John Healy of the GM Fuel Cell Activity Program.

Sample Preparation. Experiments were performed on “as received” membranes or on membranes partially neutralized by Cu(II) as CuCO_3 or CuCl_2 , Fe(II) as FeSO_4 , and Fe(III) as FeCl_3 . Neutralized membrane pieces were placed in quartz sample tubes and connected to, and sealed under, vacuum. All UV irradiations were performed at 77 K with a low-pressure mercury source (Mineralight Model PCQX1). Typical irradiation times were in the range 10–60 min. In some experiments, membranes were soaked in aqueous solutions of H_2O_2 prior to evacuation and UV irradiation.

ESR Measurements. Spectra were acquired with the Bruker X-band EMX spectrometer operating at 9.7 GHz with 100 kHz magnetic field modulation and equipped with the Acquisit 32 Bit WINEPR data system version 3.01 for acquisition and manipulation, and the ER 4111 VT variable-temperature units. Only one spectrum (Figure 7B) was measured at Q-band (34 GHz). Isotropic ESR spectra were simulated by use of the automatic optimization software WinSim version 0.96, from the National Institute of Environmental Health Sciences (NIEHS). Simulation of powder spectra was performed by use of SimFonia (Bruker) with manual parameter optimization.

Results and Discussion

Nafion/Cu(II). Typical ESR signals at the indicated temperatures of Cu(II) in Nafion membranes (degree of neutralization 2%, by CuCl_2) are presented in Figure 1. The magnetic parameters given in the figure were read directly from the spectrum

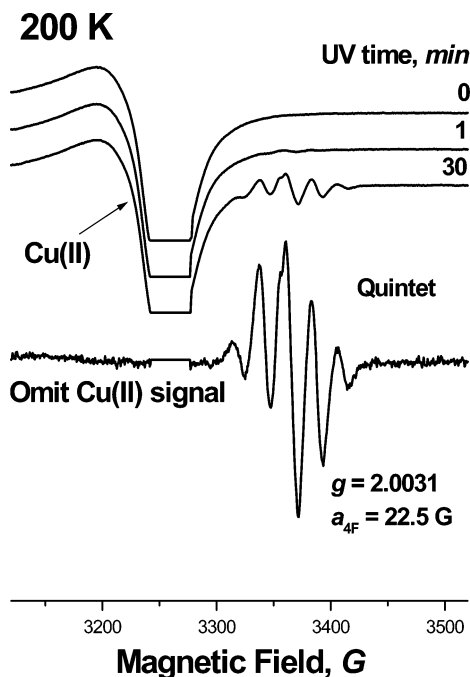


Figure 2. Evolution of the “quintet” ESR spectrum at 200 K as a function of UV irradiation time in Nafion 10% neutralized by CuCO_3 and evacuated for 1 day prior to irradiation.

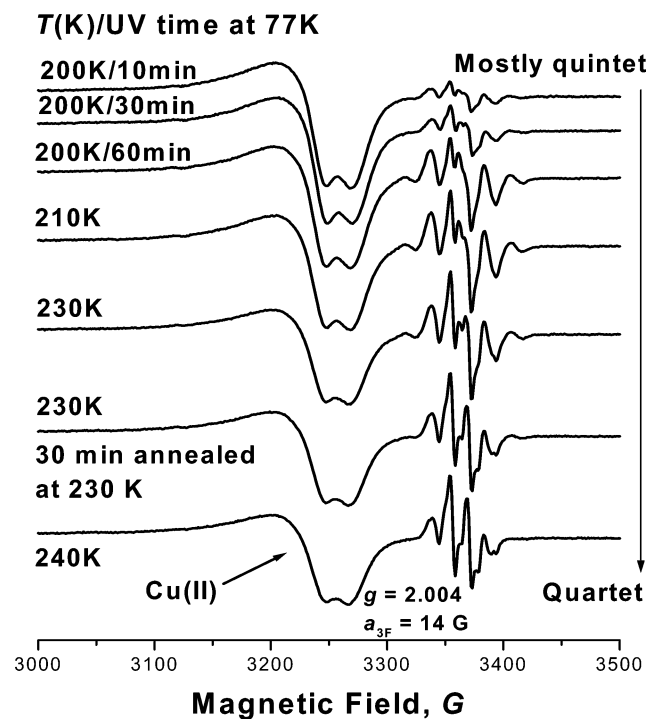


Figure 3. Transformation of the “quintet” detected in the sample described in Figure 2 into the “quartet” ESR spectrum upon annealing above 200 K.

measured at 120 K and are in accord with previous data.¹⁷ Similar signals were detected for membranes neutralized by CuCO_3 . Changes in the ESR spectra at 200 K upon UV irradiation are presented in Figure 2: the gradual formation of the “quintet” signal is seen with increasing irradiation time. The five lines are approximately in the ratio 1:4:6:4:1, as expected for hyperfine splittings (hfs) from four equivalent nuclei with $I = 1/2$, and isotropic coupling $a_{\text{iso}} = 22.5$ G. Annealing above 200 K led to the formation of the “quartet” signal, as seen in Figure 3; the new signal can be assigned to hfs from three

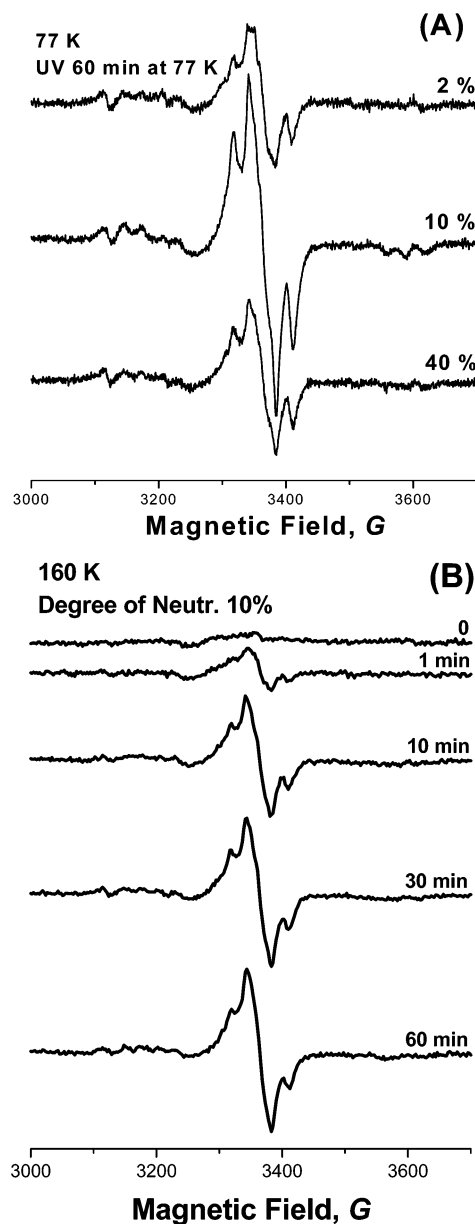


Figure 4. Formation of the chain-end radical $\text{ROCF}_2\text{CF}_2^\bullet$ in Nafion/Fe(II) as a function of (A) degree of neutralization of the membrane and (B) UV irradiation time.

equivalent nuclei with $I = 1/2$ and $a_{\text{iso}} \approx 14$ G. The quartet was also detected in Nafion/Fe(II) and the additional small splittings (≈ 5 G) of each line were assigned to spin flip satellites from neighboring protons, vide infra. Arguments for the assignments of the hfs for the quintet and quartet signals to splittings from ^{19}F nuclei will be presented below.

Nafion/Fe(II) and Nafion/Fe(III). In Nafion neutralized by Fe(II) as FeSO_4 , weak ESR signals from Nafion-derived radicals were detected at 77 K even in the absence of H_2O_2 , as seen in Figure 4. The degree of neutralization is an important factor that determined the signal intensity; in the range 2–40%, signals were strongest for 10% neutralization, as shown in Figure 4A. The signal intensity increased with irradiation time, Figure 4B; it is remarkable, however, that a weak signal was detected even in nonirradiated samples, as seen in the top spectrum in Figure 4B. This result is important because it validates the method used to form the radicals: the role of UV irradiation is therefore to accelerate the formation of a signal that is produced, albeit slowly, even in the dark and possibly during fuel cell operation.

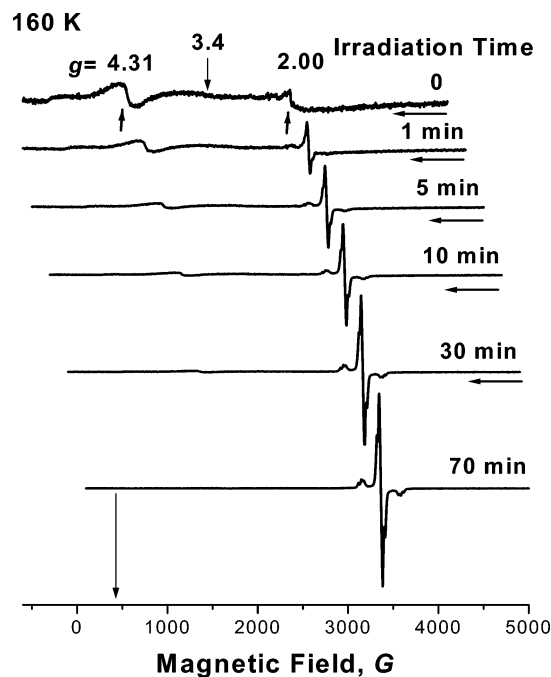


Figure 5. Effect of UV irradiation time on the intensity of the chain-end radical $\text{ROCF}_2\text{CF}_2^\bullet$ measured at 160 K in Nafion/Fe(II)/ H_2O_2 . Degree of neutralization: 40%. Note the progressive horizontal displacement of the spectra to the left, to better visualize the signal from the perfluorinated fragment.

The ESR intensity was significantly higher when the ionomer was treated with aqueous H_2O_2 prior to evacuation and UV irradiation, as seen in Figure 5. By comparison with published data on fluorinated radicals obtained by γ -irradiation or photolysis of fluorinated compounds, including poly(tetrafluoroethylene) (PTFE, Teflon),^{18–22} the signal shown in Figure 5 was assigned to the chain-end perfluorinated radical $\text{ROCF}_2\text{CF}_2^\bullet$. The presence of Fe(III) is clearly seen in Figure 5, at $g = 4.31$ and 2.00, for possible tetrahedral and octahedral coordination, respectively;^{23–26} the weak signal from octahedrally coordinated Fe(II) at $g \approx 3.4$ is also present.²⁷ As seen in Figure 6, the intensity of signals attributed to $\text{ROCF}_2\text{CF}_2^\bullet$ increases with irradiation time, while that of Fe(III) decreases. It is clear that the presence of Fe(III) is crucial for the formation of the radical. To prove this point we examined Nafion membranes that were partially neutralized by Fe(III); in these membranes strong signals from $\text{ROCF}_2\text{CF}_2^\bullet$ radicals were detected upon UV irradiation in the absence of H_2O_2 , thus providing additional proof for the conclusion that Fe(III) reacts with the membranes to form the radicals. Identical ESR signals from the $\text{ROCF}_2\text{CF}_2^\bullet$ radicals were also detected in the UV-irradiated Dow membranes that were partially neutralized by Fe(III). The results are presented in Figure 7A, which shows X-band ESR spectra at 77 K in UV-irradiated Nafion/Fe(II)/ H_2O_2 and Nafion/Fe(III), together with the simulated spectrum for the $\text{ROCF}_2\text{CF}_2^\bullet$ fragment. The ESR spectrum was simulated based on hfs from four ^{19}F nuclei, two in α and two in β positions. The magnetic parameters used for the simulation are shown in Table 1. Comparison of ESR spectra measured at 133 K at X- and Q-bands (Figure 7B) indicates that the spectrum is dominated by hyperfine splitting from ^{19}F and not by g -anisotropy, as reflected in the magnetic parameters. It is clear that the weak signals observed in Nafion/Fe(II) in the absence of H_2O_2 (Figure 4) are due to partial oxidation of Fe(II) to Fe(III), which is a facile process.

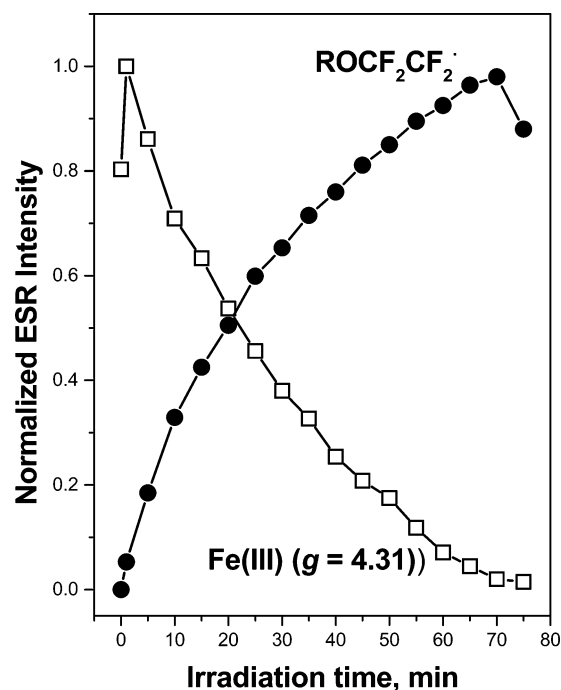


Figure 6. Increase of the chain-end radical $\text{ROCF}_2\text{CF}_2^\bullet$ intensity in Nafion/Fe(II)/ $\text{H}_2\text{O}_2/\text{H}_2\text{O}$ and decrease of the Fe(III) signal with irradiation time. Degree of neutralization: 40%.

TABLE 1: Magnetic Parameters of the Chain-End Radical $\text{ROCF}_2\text{CF}_2^\bullet$ in Nafion^a

$g_{xx} = 2.0023$	$g_{yy} = 2.0023$
$g_{zz} = 2.0030$	$g_{iso} = 2.0025$
$n(\text{F}_\alpha) = 2$	$n(\text{F}_\beta) = 2$
$A_{xx}(\text{F}_\alpha) = A_{yy}(\text{F}_\alpha) = 18 \text{ G}$	$A_{xx}(\text{F}_\beta) = A_{yy}(\text{F}_\beta) = 38 \text{ G}$
$A_{zz}(\text{F}_\alpha) = 222 \text{ G}$	$A_{zz}(\text{F}_\beta) = 30 \text{ G}$
$a_{iso}(\text{F}_\alpha) = 86 \text{ G}$	$a_{iso}(\text{F}_\beta) = 35 \text{ G}$

^a $n(\text{F}_\alpha)$ and $n(\text{F}_\beta)$ are the number of α and β interacting ^{19}F nuclei, respectively. The simulation is based on Gaussian line shapes, line widths 38 G (x, y), and 18 G (z), $\theta = 100$, and $\varphi = 1$.

The line shape variation with temperature in the range 77–260 K is shown in Figure 8. The lines gradually broaden and the resolution in the wings, which is due to hfs from F_β nuclei, decreases and is lost at $\approx 170 \text{ K}$; at 260 K the spectrum is dominated by the isotropic hfs from the F_α nuclei, $a_{iso}(\text{F}_\alpha) = 86 \text{ G}$ (Table 1) and $g_{iso} = 2.0020$.

For some combinations of temperature, degree of neutralization by Fe(II), and $\text{ROCF}_2\text{CF}_2^\bullet$ and (low) H_2O_2 concentrations, the signal from the chain-end radical is transformed into the “quartet”, as seen in Figure 9; this signal is identical to that detected in Nafion/Cu(II) (Figure 3). The ESR spectrum of the quartet is shown more clearly in Figure 10A: signals shown by arrows are clearly from interacting protons, as they disappeared when the radical was formed in Nafion/Fe(II)/ $\text{H}_2\text{O}_2/\text{D}_2\text{O}$ (Figure 10B). Simulation of the spectra allowed a more accurate determination of the main splittings (14.2 G). The hyperfine splitting from protons, $a_H \approx 5 \text{ G}$, are spin-flip satellites; as expected,²⁸ their intensity increased with increasing microwave power.

Magnetic Parameters of the Chain-End Radical $\text{ROCF}_2\text{CF}_2^\bullet$. The principal values of the g - and ^{19}F hyperfine tensors given in Table 1, obtained by simulation of the ESR spectrum from the chain-end radical, can be compared with literature values.^{18–22} The principal values of the hyperfine tensor of the F_α nuclei in the $\text{ROCF}_2\text{CF}_2^\bullet$ radical are 222, 18, and 18 G, close to the corresponding values of 225, 17, and 17 G determined for the propagating chain-end radical in PTFE.^{19,21} The isotropic

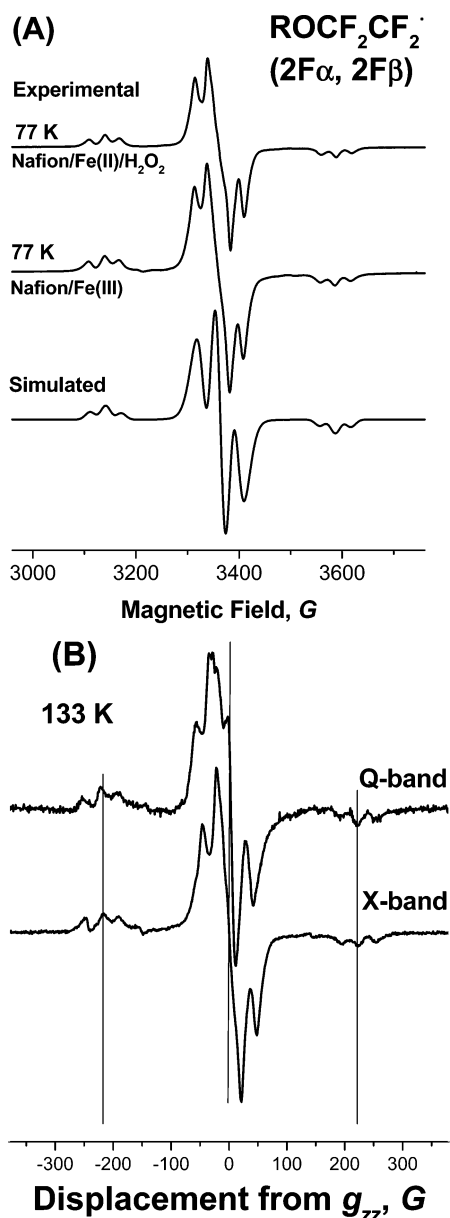


Figure 7. (A) ESR spectrum at 77 K of the chain-end radical $\text{ROCF}_2\text{CF}_2^*$ in UV-irradiated Nafion/Fe(II)/ $\text{H}_2\text{O}_2/\text{H}_2\text{O}$ (60 min, degree of neutralization 40%) and in UV-irradiated Nafion/Fe(III) (55 min, degree of neutralization 10%) and the corresponding simulated spectrum. The magnetic parameters used in the simulation spectrum are given in Table 1. (B) Comparison of ESR spectra at X-Band and Q-band (34 GHz), $T = 133$ K.

splitting, $a_{\text{iso}} = 86$ G, is identical in both systems and close to the value of 87.3 G measured for the fragment $\text{ROCF}_2\text{CF}_2^*$ detected in the high-temperature photolysis of perfluorinated polyethers.²²

The principal values of the hyperfine tensor for the F_β nuclei in the $\text{ROCF}_2\text{CF}_2^*$ radical in Nafion are 30, 38, and 38 G ($a_{\text{iso}} = 35$ G), different compared to the corresponding values of 10, 17, and 17 G ($a_{\text{iso}} = 15$ G) determined for the propagating chain-end radical in PTFE. The larger and less anisotropic values for the chain-end radical in Nafion led to an exceptionally well-resolved spectrum, especially in the wings, and even at low temperature (77 K, Figure 7A). The principal values determined for the F_β nuclei in the Nafion-derived radical can also be compared with the values of 67, 25, and 21 G ($a_{\text{iso}} = 38$ G) for $^*\text{CF}(\text{COO}^-)\text{CF}_2\text{COO}^-$ trapped in sodium perfluorosuccinate.^{18,20a} The similarity of the a_{iso} values in Nafion and sodium

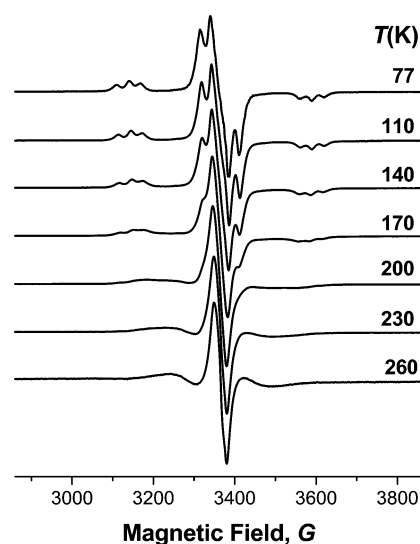


Figure 8. Temperature dependence of signal from the chain-end radical $\text{ROCF}_2\text{CF}_2^*$ in UV-irradiated Nafion/Fe(II)/ $\text{H}_2\text{O}_2/\text{H}_2\text{O}$.

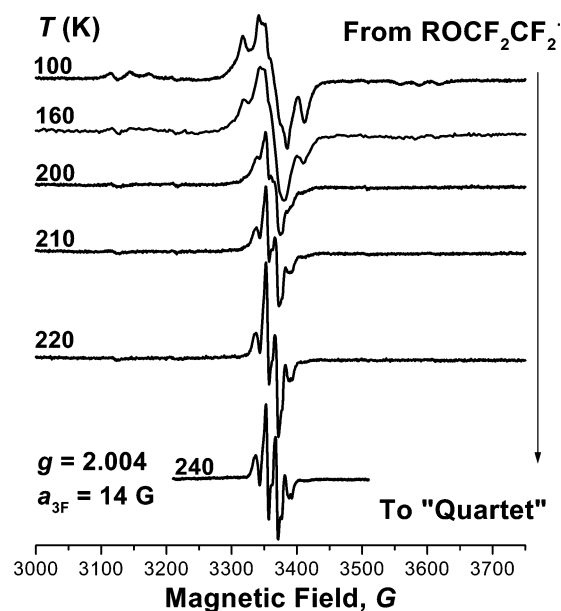


Figure 9. Transformation of the chain-end radical $\text{ROCF}_2\text{CF}_2^*$ in Nafion/Fe(II)/ $\text{H}_2\text{O}_2/\text{H}_2\text{O}$ into the "quartet", with hyperfine splittings from three ^{19}F nuclei. Degree of neutralization: 10%.

perfluorosuccinate suggests a similar conformation of the radicals. Isotropic hyperfine splittings from β nuclei are sensitive to the radical conformation and usually follow

$$a_{\text{iso}}(F_\beta) = b_1 + b_2 \cos^2 \theta \quad (1)$$

where θ is the dihedral angle, between the direction of the unpaired electron and the projection of the $\text{C}_\beta\text{--F}_\beta$ bond on a plane perpendicular to the direction of the $\text{C}_\alpha\text{--C}_\beta$ direction. For ^{19}F nuclei, $b_1 \approx 0$, and b_2 is known to vary in the range 50–80 G, depending on the particular system.²⁰ On the basis of $b_2 \approx 65$ G, we obtain $\theta = 43^\circ$ for the chain-end radical in Nafion, compared to 61° in the propagating chain-end radical in PTFE. The large difference in the dihedral angle for these two systems strongly suggests that the radical in Nafion is not part of the backbone. We propose the radical structure and conformation shown in Figure 11.

A possible route for the radical formation is UV scission of the C–S bond in the pendant chain of Nafion. The weak signal

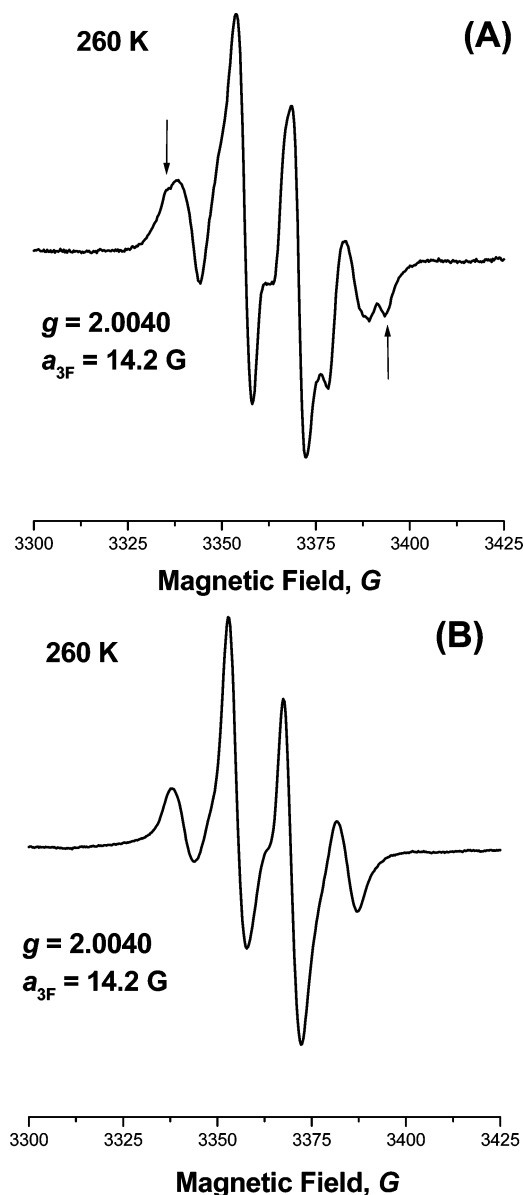


Figure 10. ESR spectra at 260 K of the “quartet” radical in (A) Nafion/Fe(II)/H₂O₂/H₂O and (B) Nafion/Fe(II)/H₂O₂/D₂O. Arrows in panel A point to splittings from ¹H nuclei. Degree of neutralization: 10%.

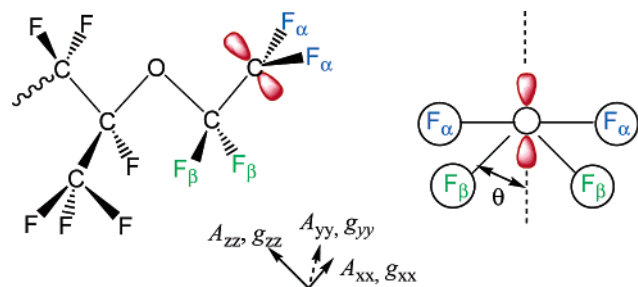


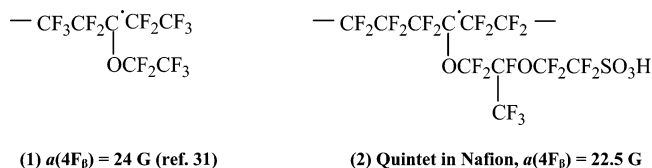
Figure 11. Proposed structure and conformation of the ROCF₂CF₂· radical fragment detected in Nafion, and the directions of the principal values of the ¹⁹F hyperfine- and *g* tensors. The 2p π orbital of the unpaired electron is shown in red and θ is the dihedral angle, equal to $\approx 43^\circ$.

detected in Nafion/Fe(II) in the absence of H₂O₂ (Figure 4) and the strong signal in the presence of H₂O₂ (Figure 5) suggest that Fe(III) facilitates such scission; the decrease of the Fe(III) signal in parallel to the increased intensity from the ROCF₂-CF₂· radical is additional confirmation for the important role

of Fe(III). The process we propose is $\text{-OCF}_2\text{CF}_2\text{SO}_3^- + \text{Fe(III)} \rightarrow \text{-OCF}_2\text{CF}_2\text{SO}_3^\bullet + \text{Fe(II)}$.²⁹ Recombination of $\text{-OCF}_2\text{-CF}_2\text{SO}_3^\bullet$ radicals can lead to SO₂, O₂, and the chain-end radical $\text{-OCF}_2\text{CF}_2^\bullet$. We note that in the case of UV-irradiated lead [Pb(IV)] alkanoates, the initial process was identified as scission of the Pb–O bond followed by rapid decarboxylation, leading to radicals of the type RCF₂CF₂·, where R is F or CF₃.³⁰ A similar process could also be valid for Nafion, with desulfonation replacing decarboxylation.

Quartet and Quintet Radicals. These radicals could also be formed in reactions involving the chain-end $\text{-OCF}_2\text{CF}_2\text{SO}_3^\bullet$ species. It is reasonable to assume that the quartet signal, which is formed by the disappearance of the perfluorinated chain-end radical in Nafion/Fe(II)/H₂O₂ and was detected in Nafion/Cu(II), is also a perfluorinated radical. Isotropic hyperfine splittings from three fluorine atoms, with $a_{\text{iso}} = 14.2$ G and $g_{\text{iso}} = 2.004$, were deduced by simulation. The g_{iso} value suggests a carbon-centered radical. The isotropic hfs in both quartet and quintet radicals are too low to arise from radicals where the unpaired electron is centered on the carbon in a C–F fragment; $\text{-C}\cdot\text{O}$ fragments, with no α fluorine nuclei, are more likely candidates. We note that a radical showing interactions with three β fluorine nuclei and $a_{\text{iso}} = 11.5$ G was assigned to the radical CF₃C·O, a value similar to that in the quartet radical in Nafion.³¹

The quartet is formed in Nafion/Cu(II) by the transformation of the quintet radical, with $a_{\text{iso}} = 22.5$ G. A similar quintet ($a_{\text{iso}} = 24$ G) was detected during the photolysis of perfluoroketones and assigned to radical **1** below.³¹ By analogy, we propose radical **2** below as responsible for the quintet detected in Nafion. Structure **2** implies that the unpaired electron is located on the carbon atom in the Nafion backbone that is linked to the pendant chain by loss of a fluorine atom. This structure is in agreement with the detection of F[−] anions during fuel cell operation.³²



The proton spin flip satellites detected for the quartet (Figure 10) also suggest the proximity of the pendant side chain to the radical; the proton could come from water protons or from nonneutralized sulfonic groups. More work, including DFT calculations, is planned to clarify the assignments of these quartet and quintet radical fragments.

This study has emphasized the major role played by the cations used for membrane neutralization in membrane stability. The active role played by the counterions in radical formation suggests that the point of attack is at or near the ionomer side chain. Recent degradation studies on perfluorinated membranes treated by the Fenton reagent have suggested that degradation due to oxygen radicals starts at the chain end of the ionomer, propagates along the main chain, and releases side-chain fragments.³² The present study suggests an alternative mechanism for the formation of membrane-derived fragments, which involves Cu(II) and Fe(III).

Conclusions

The most surprising aspect of this study was the formation of membrane-derived radical species only in the neutralized membranes, and even in the absence of H₂O₂ in the case of

Nafion/Cu(II) and Nafion/Fe(III). This result suggests involvement of the cations in degradation processes.

The different behavior of Cu(II) and Fe(II) or Fe(III) is also a major result. The formation of Fe(III) in Nafion/Fe(II)/H₂O₂, visible through the signals corresponding to $g = 4.3$, and to 2.00 in Figure 5, and the consumption of Fe(III) in parallel to the formation of the chain-end radical ROCF₂CF₂• (Figure 6) indicated participation of Fe(III) in scission and/or redox reactions. The chain-end radical can be formed by UV scission of the C–S bond in the Nafion pendant chain and/or by the reaction $\text{-OCF}_2\text{CF}_2\text{SO}_3^- + \text{Fe(III)} \rightarrow \text{-OCF}_2\text{CF}_2\text{SO}_3^\bullet + \text{Fe(II)}$; radicals $\text{-OCF}_2\text{CF}_2\text{SO}_3^\bullet$ can recombine to form SO₂, O₂, and the chain-end radical $\text{-OCF}_2\text{CF}_2^\bullet$. The formation of the radical quintet may suggest attack of the carbon backbone atom linked to the pendant chain and loss of an F atom. The presence of the quartet may signal formation of smaller fragments, derived as well from the pendant chain.

This study has indicated that when studying membrane stability, it is important to consider not only the formation of oxygen radicals but also the reactivity of counterions.

Acknowledgment. This study was supported by General Motors Fuel Cell Activities Program and by the Polymers Program of NSF. Experiments at the National Biomedical EPR Center, Medical College of Wisconsin in Milwaukee, WI, were supported by Grant EB001980. We are grateful to Christofer C. Felix and William Antholine for their help with the Q-band ESR experiments in Milwaukee; to Dennis E. Curtin of DuPont Company for the gift of Nafion membranes; to John Healy of General Motors for the gift of Dow membranes; and to Mariana Pinteala, John Healy, and Charlene Hayden (GM) for illuminating discussions on radical formation in the perfluorinated membranes. We are thankful to one referee for careful reading, constructive criticism, and useful suggestions on improving the manuscript.

References and Notes

- (1) Risen, W. M., Jr. In *Ionomers: Characterization, Theory, and Applications*; Schlick, S., Ed.; CRC Press: Boca Raton, FL, 1996; Chapt. 12, pp 281–300.
- (2) Gasteiger, H. A.; Mathias, M. F. *Proceedings of the Symposium on Proton Conducting Membrane Fuel Cells III*; Murthy, M., Fuller, T. F., Van Zee, J. W., Eds.; Salt Lake City, 2002, The Electrochemical Society, Vol. PV 2002-31, in press.
- (3) Huang, C.; Tan, K. S.; Lin, J.; Tan, K. L. *Chem. Phys. Lett.* **2003**, 371, 80.
- (4) Schmidt, T. J.; Paulus, U. A.; Gasteiger, H. A.; Behm, R. J. *J. Electroanal. Chem.* **2001**, 508, 41 and references therein.
- (5) Lu, C.; Rice, C.; Masel, R. I.; Babu, P. K.; Waszczuk, P.; Kim, H. S.; Oldfield, E.; Wieckowski, A. *J. Phys. Chem. B* **2002**, 106, 9581.
- (6) Walling, C. *Acc. Chem. Res.* **1975**, 8, 125.
- (7) Bednarek, J.; Schlick, S. *J. Phys. Chem.* **1991**, 95, 9940.
- (8) Miyatake, K.; Oyaizu, K.; Tsuchida, E.; Hay, A. S. *Macromolecules* **2001**, 34, 2065.
- (9) Fang, J.; Guo, X.; Harada, S.; Watari, T.; Tanaka, K.; Kita, H.; Okamoto, K. *Macromolecules* **2002**, 35, 9022.
- (10) Hubner, G.; Roduner, E. *J. Mater. Chem.* **1999**, 9, 409.
- (11) Panchenko, A.; Dilger, H.; Kerres, J.; Hein, M.; Ulrich, A.; Kaz, T.; Roduner, E. *Phys. Chem. Chem. Phys.* **2004**, 5, 2891.
- (12) Bosnjakovic, A.; Schlick, S., to be published.
- (13) Bosnjakovic, A.; Schlick, S. *J. Phys. Chem. B* **2004**, 108, 4332.
- (14) Alonso-Amigo, M. G.; Schlick, S. *J. Phys. Chem.* **1989**, 93, 7526.
- (15) Dubinsky, S.; Grader, G. S.; Shter, G. E.; Silverstein, M. S. *Polym. Degrad. Stab.* **2004**, 86, 171.
- (16) Pozio, A.; Silva, R. F.; De Francisco, M.; Giorgi, L. *Electrochim. Acta* **2003**, 48, 1543.
- (17) Alonso-Amigo, M. G.; Schlick, S. *J. Phys. Chem.* **1986**, 90, 6353.
- (18) Rogers, M. T.; Whiffen, D. H. *J. Chem. Phys.* **1964**, 40, 2662.
- (19) (a) Toriyama, K.; Iwasaki, M. *J. Phys. Chem.* **1969**, 73, 2919. (b) *J. Chem. Phys.* **1969**, 73, 2663.
- (20) (a) Kispert, L. D.; Rogers, M. T. *J. Chem. Phys.* **1971**, 54, 3326. (b) Bogan, C. M.; Kispert, L. D. *J. Phys. Chem.* **1973**, 77, 7, 1491–1496. (c) Kispert, L. D. In *Fluorine-Containing Free Radicals: Kinetics and Dynamics of Reactions*; Root, J. W., Ed.; ACS Symposium Series 66; American Chemical Society: Washington, DC, 1978; Chapt. 13, pp 349–385.
- (21) (a) Hara, S.; Yamamoto, K.; Shimada, S.; Nishi, H. *Macromolecules* **2003**, 36, 5661. (b) *J. Polym. Sci. Polym. Phys. Ed.* **2004**, 42, 1539.
- (22) Faucitano, A.; Buttafava, A.; Martinotti, F.; Marchionni, G.; De Pasquale, R. *J. Tetrahedron Lett.* **1990**, 31, 7055 and references therein.
- (23) Goldfarb, D.; Bernardo, M.; Strohmaier, K. G.; Vaughan, D. E. W.; Thomann, H. *J. Am. Chem. Soc.* **1994**, 116, 6344.
- (24) Wloch, E.; Sulikowski, B.; Dula, R.; Serwicka, E. M. *Colloids Surf. A: Physicochem. Eng. Aspects* **1996**, 115, 257.
- (25) Bruckner, A.; Lohse, U.; Mehner, H. *Microporous Mesoporous Mater.* **1998**, 20, 207.
- (26) Hunger, M.; Weitkamp, J. *Angew. Chem., Int. Ed.* **2001**, 40, 2954.
- (27) McGarvey, B. R. In *Transition Metal Chemistry*; Carlin, R. L., Ed.; Marcel Dekker: New York, 1966; Vol. 3, pp 89–201.
- (28) (a) Schlick, S.; Kevan, L. *J. Magn. Reson.* **1976**, 21, 129. (b) *J. Magn. Reson.* **1976**, 22, 171 and references therein.
- (29) Allcock, H. R.; Lampe, F. W.; Mark, J. E. *Contemporary Polymer Chemistry*, 3rd ed.; Pearson/Prentice Hall: Upper Saddle River, NJ, 2003; p 65.
- (30) Ayscough, P. B.; Machova, J.; Mach, K. *J. Chem. Soc., Faraday Trans. 2* **1973**, 69, 750.
- (31) Krusic, P. J.; Chen, K. S.; Meakin, P.; Kochi, J. K. *J. Phys. Chem.* **1974**, 78, 8, 2036.
- (32) Healy, J.; Hayden, C.; Xie, T.; Olson, K.; Waldo, R.; Brundage, M.; Gasteiger, H.; Abbott, J. Published Online Nov. 23, 2004, DOI: 10.1002/fuce.200400050.